Uses of Usumacinta River sediments as a sustainable resource for unpaved roads: an experimental study on a full-scale pilot unit

Irini Djeran-Maigre, Ahmad Morsel, L. Briancon, Estelle Delfosse, Daniel Levacher, Andry Razakamanantsoa

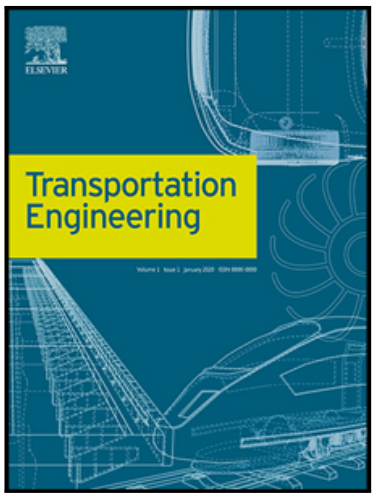

Uses of Usumacinta River sediments as a sustainable resource for unpaved roads: an experimental study on a full-scale pilot unit

I. Djeran-Maigre , A. Morsel , L. Briançon , E. Delfosse ,
D. Levacher , A.R. Razakamanantsoa

PII: S2666-691X(22)00034-3
DOI: https://doi.org/10.1016/j.treng.2022.100136
Reference: TRENG 100136

To appear in: *Transportation Engineering*

Received date: 10 May 2022
Revised date: 20 July 2022
Accepted date: 8 August 2022

Please cite this article as: I. Djeran-Maigre , A. Morsel , L. Briançon , E. Delfosse , D. Levacher , A.R. Razakamanantsoa , Uses of Usumacinta River sediments as a sustainable resource for unpaved roads: an experimental study on a full-scale pilot unit, *Transportation Engineering* (2022), doi: https://doi.org/10.1016/j.treng.2022.100136

Highlights

- Raw and lime-treated sediments characterization (51)
- Reconstitutions of untreated and lime-treated soil-models (60)
- Cyclic loading plate and traffic testing on a full-scale pilot with soil-models (82)
- Soil-model behavior and full-scale pilot results are very promising (70)
- Suitability of Usumacinta sediments as unpaved road material demonstrated (76)

Use of Usumacinta River sediments as a sustainable resource for unpaved roads: an experimental study on a full-scale pilot unit

Djeran-Maigre I.[1*], **Morsel A.**[1,4], **Briançon L.**[1], **Delfosse E.**[1], **Levacher D.**[2], **Razakamanantsoa A.R.**[3]

[1] Univ Lyon, INSA Lyon, GEOMAS, EA7495, 69621 Villeurbanne, France

[2] Normandie Université, Unicaen, UMR 6143 CNRS-M2C, 14000 Caen, France

[3] Université Gustave Eiffel, Département GERS-GIE, 44344 Bouguenais, France

[4] ECN, Laboratory GeM, UMR 6183, 44300 Nantes, France

*Corresponding author

Abstract

Purpose: Transportation is a key factor for economic growth and poverty reduction because it improves access to services and opportunities for rural communities. Unpaved roads, however, still represent 80% of the global road network. The state of Tabasco, Mexico, is not an exception.

Materials and methods:

Geotechnical identifications of raw and lime-treated sediments are performed. A methodology is developed to reproduce a soil-model close to the raw sediment's properties. The reconstituted soil-model is used for full-scale testing including CBR indexes determination, cyclic vertical plate testing and horizontal traffic loads tests.

Results: The rutting generated from the cyclic plate and traffic load tests, on both the untreated and the lime-treated soil-model, are compared. The lime treatment appears to improve the properties of both the soil-model and the sediments.

Conclusions: The findings give promising perspectives regarding the use of Usumacinta River sediments for the construction of unpaved roads.

Key Words:

Usumacinta River sediments, lime treatment, soil-model, cyclic plate testing, traffic load testing, unpaved road, full-scale pilot unit, rutting depth

Introduction

The present study is part of a broader joint research project conducted to investigate the adaptation of the Usumacinta River Basin (Mexico) in the context of global change and ecological transition. The objective of the project is to examine the socio-ecosystem of this basin through its sediments and propose a solution for an integrated valorisation of these sediments that could benefit the local population [1]. The Usumacinta River runs through the state of Tabasco, one of the poorest and most rural states in Mexico [2].

Transportation and more specifically rural transport is a crucial lever for economic growth and poverty reduction and will contribute to the achievement of the Millennium Development Goals [3]. Despite the fact that unpaved roads made of earth or gravel account for 80 percent of the global road network and 90 percent of rural roads in developing regions, and that many communities rely on these roads for access, little research has been conducted on the subject of unpaved roads until now [4]. Many authors have studied the factors causing erosion, a key problem affecting unpaved roads [5, 6, 7, 8]. On the other hand, a survey of the literature reveals that little effort has been devoted to the subject of the rutting (longitudinal surface depression in the wheel path). The few studies addressing the problem of road traffic effects on the formation of wheel ruts, mainly focus on geotextile-reinforced unpaved roads [9, 10, 11].

Moreover, because unpaved roads are regularly experiencing periods of heavy traffic or adverse weather conditions, they require regular maintenance. The lack of maintenance, truck overloads are directly responsible for the deterioration of roads, which may become impassable after heavy rain periods. Climate change is worsening this situation because many rural regions with unpaved roads experience increasing extreme rainfall events [12].

Resources for unpaved road transport infrastructures are usually scarce with very limited support from central governments or other external sources [13]. Under these conditions, sustainable rural road technology should be: 1) simple and easy to implement with minimal on-site supervision; 2) robust enough to remain serviceable with no need for regular and recurring maintenance; 3) inexpensive and prioritize locally available materials, and 4) able to be maintained by locals with minimal training [4]. Consequently, the use of a locally available material that is inexpensive and requires little transportation is particularly relevant.

With a total length of 223,237 km, the Mexican unpaved road network represents almost 60% of the total road network [14, 15]. In the Usumacinta River Basin, the proximity of the river and the presence of sediments could respond to the issue of providing local and low-cost materials to build sustainable rural earth roads and ensure easy maintenance. Indeed, many studies have shown that using marine and river sediments as materials for road construction is possible [16, 17, 7, 18, 19, 20]. Levacher [21], in particular, have proposed criteria based on the geotechnical, physico-chemical and contamination characteristics of the sediments to determine whether the sediments are suitable for use in road construction.

However, dredged sediments generally do not meet material specifications because of high-water contents and relatively poor mechanical performances [22]. Consequently, stabilisation using hydraulic binders or lime is necessary to enhance the properties of the sediments [23, 24, 25]. Most investigations on the valorisation of dredged sediments for road construction draw their conclusions from laboratory tests [26, 27, 28, 29]. Only a few studies investigate the behavior of in-situ roads built with a sub-base layer of dredged sediments [30, 31]. However, the mechanical performances of the road have been investigated through sampling and laboratory testing. To our knowledge, there are no full-scale studies dealing specifically with the effects of traffic loading on a dredged sediment-based road.

The objectives of this study are multiple:
The Usumacinta sediments are investigated for identification purposes. A soil-model (SM) representative of these sediments properties is formulated. A full-scale pilot, for unpaved roads is constructed: untreated (SM) and lime-treated soil-model (TSM) are tested under different solicitations. Three experimental programs are proposed to study: material workability, traffic resistance and vertical loading resistance. The behavior of the materials with respect to the applied loads is evaluated. The methodological approach developed is expected to be reproduced on the Mexican sediments of Usumacinta for unpaved road design and construction.

1. Study areas and sediment characteristics of the Usumacinta River

1.1. Location and sediment sampling

The sediments come from the Usumacinta River, a 1,000 km-long river that runs through the state of Tabasco, Mexico (Figure 1). The sediments have been sampled from upstream of Tenosique and downstream of Jonuta, two cities in Tabasco state along the river. In these two cities, the geomorphological characteristics of the river are distinct, and the sediments have origin-dependent characteristics. Sediments have been collected at five and four different locations in Tenosique and in Jonuta respectively,portable sampling systems (cone samplers, shovels, buckets). The saturated samples have then been stored in airtight barrels and transported to France by boat. They are labelled with the letters T (for Tenosique) or J (for Jonuta) and a number corresponding to the site where they have been collected.

Figure 1 : a) State of Tabasco in Mexico,
b) Usumacinta River in the State of Tabasco and sampling sites

1.2. Environmental impact

Prior to recycling, the possibility of the use of Usumacinta sediments depends on their pollution level. The chemical analyses of sediments show that the concentrations of Polycyclic Aromatic Hydrocarbons (PAHs), PolyChlorinated Biphenyls (PCBs), heavy metals, volatile compounds, chlorophenols, and glyphosates are less than the regulatory thresholds, recommended for continental sediments in France [32]. Only nickel (Ni)

concentration is slightly higher and specific treatment can be recommended before any beneficial use.

2. Materials

2.1. Usumacinta River sediments

2.1.1. Raw sediments

The first objective of this study is to examine the ability of Usumacinta River sediments to be used as material for unpaved road construction, according to the French guide for earthworks, [33].

Table 1 presents the particle size distribution of all the sediment samples. The samples consist primarily of silty sediment materials with a silt fraction between 41% and 85%. The percentage of fine sand varies considerably between 3.4% and 54.2%. T3 and J4 sediments that have the lowest sand content also have the highest clay content. The clay content of Usumacinta river sediments is generally low (<15%) compared to silt and sand fractions, except for T3 and J4 sediments.

Table 1: Grain size distribution of Usumacinta River sediments

	Clay (< 2.5µm) %*	Silt (2.5 – 25µm) %*	Sand (> 25 µm) %*
T1	5.80	48.10	46.10
T2	3.67	50.93	45.40
T3	11.80	84.80	3.40
T5	7.56	63.44	29.00
T6	4.72	41.08	54.20
J1	6.23	51.67	42.10
J3	6.17	47.13	46.70
J4	13.10	79.90	7.00
J5	6.39	55.81	37.80

* Results correspond to the volumetric percentage

According to the French standard [33], T1, T2, and T6 are classified as A1 (low plastic silts, loess, alluvial silts, low polluted fine sands, low plastic), and T3, T5, J1, J3, J4, and J5 are classified as A2 (low plastic fine clayey sands, silts, clays and marls) as summarized in Table 2.

Table 2: Geotechnical properties and soil classification

Sediment	Organic Matter %	% passing at 80 µm %	MBV g/100g	Atterberg Limits LL	LP	PI*	GTR classification
T1	4.7	75	2.3	39.0	31.0	8.0	A1
T2	3.5	42	1.8	33.0	22.9	10.1	A1
T3	5.0	89	3.1	49.0	36.7	12.3	A2 / A1
T5	3.6	85	5.7	40.9	25.5	15.2	A2
T6	3.5	62	2.5	55.0	(-)	(-)	A1
J1	4.5	98	4.6	52.8	33.0	19.8	A2
J3	5.1	85	3.4	43.5	30.7	12.8	A2
J4	6.0	94	7.7	62.0	43.9	18.1	A2
J5	4.9	98	4.2	45.6	33.8	11.8	A2

*Note: *PI = LL – LP with LL: Liquidity limit ; LP: Plasticity limit*
MBV: Methylene Blue Value

The compaction properties, such as maximum dry density (MDD) and optimum water content (OWC) of the sediments are measured based on the French standard [34]. The maximum dry density of all the sediments is very close with an average value of 1.6 Mg/m^3. Greater variations are observed for the optimum water content, which ranges from 18.2% to 32.3% (Table 3). Sediments T3 and J4, which have the lowest maximum dry density, also have the highest optimum water content (Figure 3a and Figure 3c). This is consistent with the fact that both have the highest clay contents.

Table 3: Maximum dry density and optimal water content of the sediments

	T1	T2	T3	T5	T6	J1	J3	J4	J5	**Avg.**
MDD (Mg/m^3)	1.7	1.6	1.3	1.7	1.7	1.6	1.6	1.5	1.6	**1.6**
OWC (%)	18.2	19.8	32.3	19.9	18.1	22.9	23.2	27.1	23.8	**2.0**

2.1.2. Lime-treated sediment

As sediments usually do not meet material specification requirements due to their high water content and relatively poor mechanical properties [22], they require special treatment to stabilise and enhance their characteristics. This also applies to A1 and A2 materials. The conventional treatment for the solidification or stabilisation of sediments is the addition of hydraulic binders or lime. Here, lime treatment is preferred for the following reasons: it is inexpensive and readily available in the Tabasco region (Mexico). Lime is also generally used to stabilise silty and clayey soils. It triggers quick changes in the geotechnical properties: the flocculation process of clay occurs within a few hours and gives the soil a granular, stable and non-sticky structure [35]. First, the sediments were treated with Mexican lime, and the

mechanical properties such as dry density, and water content were determined; then, for comparison purposes, the sediments were treated with French quicklime, a product equivalent to Mexican lime. Quicklime is also used for full-scale testing, which requires a large amont of material and because the amount of Mexican lime brought back to France was limited and not sufficient in volume.

Lime treatment first concerns the determination of the lime dosage. The lime fixation point (LFP), corresponding to the minimum lime concentration required to initiate the pozzolanic reaction, is measured for two types of lime according to the American standard [36]. It involves determining the pH of a solution of demineralized water and sediment using the formula L/S = 5, where L represents the mass of water and S represents the mass of sediment. Different percentages of lime were added to this solution and the pH was measured after 1 hour. A pH of 12.4 is required to initiate the pozzolanic reaction between sediment and lime. Thus, the minimum percentage of lime to use is the amount of lime that gives a pH of 12.4. The minimum percentage of lime required to stabilise sediments varies from 1.5% to 2%. Only sediment J4 with the highest amount of clay requires the use of a larger amount of lime (Table 4). The amounts of Mexican lime and French quicklime required are very similar and confirm that quicklime can be used as an alternative to Mexican lime for full-scale testing.

Table 4: Minimum amount in % of lime required for each sediment sample

	T1	T2	T3	T5	T6	J1	J3	J4	J5
Mexican lime (%)	2.0	1.5	2.0	1.5	1.5	2.0	2.0	3.0	2.0
French quicklime (%)	2.0	1.5	1.5	1.5	1.5	1.5	1.5	2.0	1.5

The compaction properties (MDD, OWC) of the sediments treated with the required amount of lime, are determined and presented in Figure 2b and Figure 2d.

Lime treatment is known to modify the physico-chemical properties of clay materials, notably by improving their workability, flocculation and load-bearing capacity. … As expected, a decrease in the dry density and an increase in the optimum water content are observed in the lime-treated materials (Figure 2). However, it should be noted that the decrease in the optimum dry density is relatively small and that, for sediment T2, the lime treatment has limited effect (Table 5 and Table 6). The improved properties obtained using French quicklime are very similar to those obtained using Mexican lime, thus, as said above, French quicklime can be used as a suitable alternative to Mexican lime for full-scale testing.

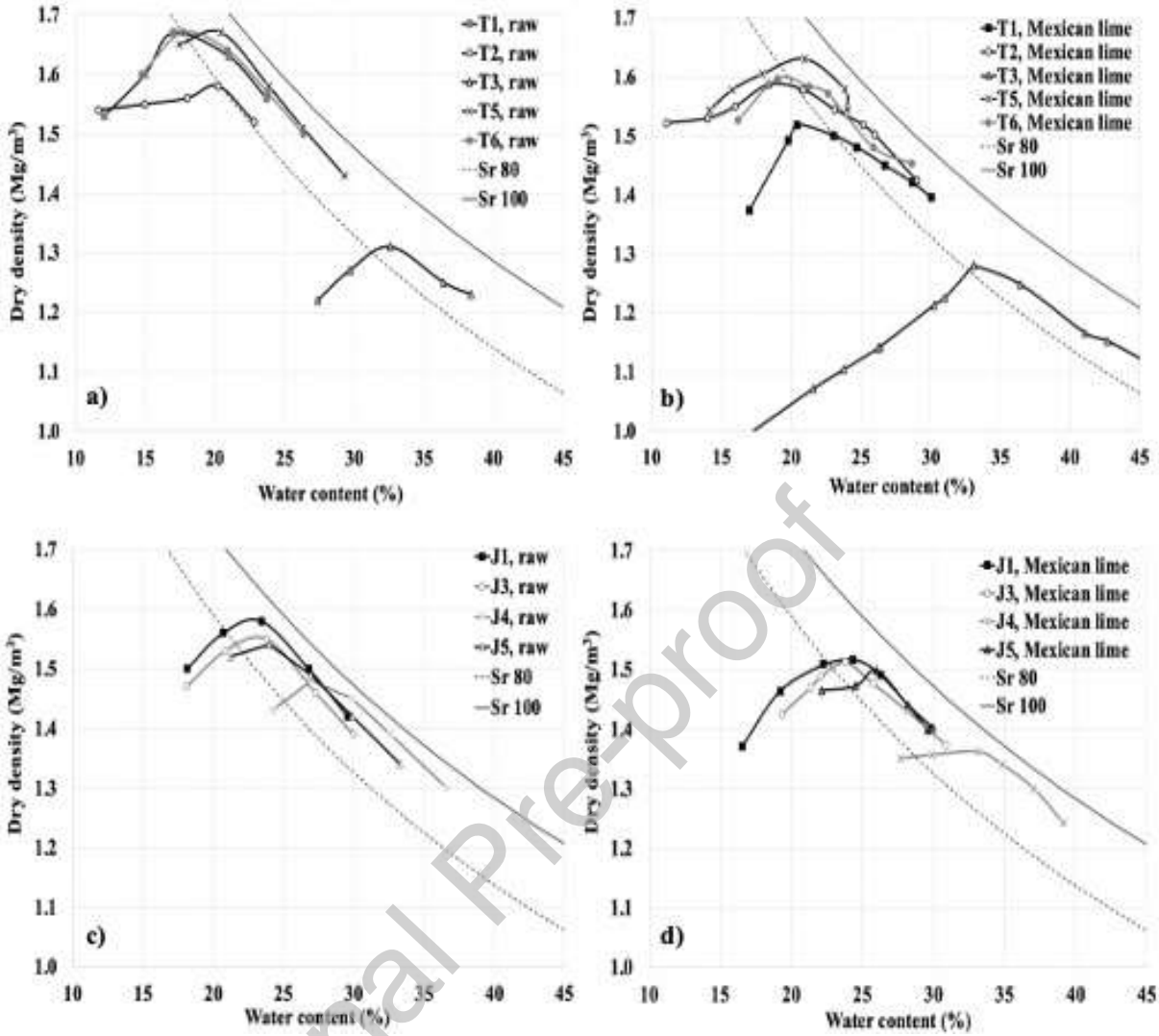

Figure 2: Standard Proctor compaction curve of: a) Tenosique raw sediment – b) Tenosique Mexican lime-treated sediment– c) Jonuta raw sediment – d) Jonuta Mexican lime-treated sediment

Table 5: Maximum dry density (Mg/m^3) of raw and lime-treated sediments

Sediment	T1	T2	T3	T5	T6	J1	J3	J4	J5	Avg.
Raw sediment	1.7	1.6	1.3	1.7	1.7	1.6	1.6	1.5	1.6	1.6
Mexican lime	1.5	1.6	1.3	1.6	1.6	1.5	1.5	1.4	1.5	1.5
French quicklime	1.5	1.6	1.3	1.6	1.6	1.5	1.5	1.4	1.5	1.5

Table 6: Optimal water content OWC in % of raw and lime-treated sediments

Sediment	T1	T2	T3	T5	T6	J1	J3	J4	J5	Avg.
Raw sediment	18.2	19.8	32.3	19.9	18.1	22.9	23.2	27.1	23.8	19.8
Mexican lime	20.4	18.4	33.1	21.0	19.1	24.3	23.8	33.1	26.0	24.4
French quicklime	22.4	19.7	33.4	22.2	20.6	23.0	23.7	31.4	22.6	24.3

The Usumacinta River sediments are classified as geotechnical class A1-A2. For their implementation, the lime treatment allows to improve their workability and this is achieved with a small quantity of lime, about 1.5% for both types of lime tested. After lime treatment, the compaction curves confirm the expected decrease of density observed on the compacted treated material, compared to the raw material.

2.2. Soil-model to obtain similar sediments properties

In the context of reasonable use of resources, reduction of the carbon footprint, and even mutualization of means of experimentation between different research centers and/or engineers, a soil-model whose geotechnical properties are representative of the sediments of the Usumacinta was proposed to defined. According to [37], the use of the soil-model is recommended thanks to its reproducibility with controlled properties. This is perfectly convenient to verify the methodology that will be implemented for the construction of unpaved roads. The behavior study of this soil-model, at the scale of the structure, allows determining accurate way the possibility of using the sediments for unpaved road applications

2.2.1. Reconstituted soil-model

Hostun sand and Speswhite kaolinite clay are combined to reconstitute a soil-model with geotechnical properties close to the Usumacinta River sediments. Different mixtures are prepared by varying the proportion of sand and kaolinite (Table 7). For each composition, a Methylene Blue Value (MBV) test is performed and the results are placed in the material classification chart of the French standard [33] (Figure 3). MBV values for kaolinite are low. Consequently, increasing the kaolinite content in the mixtures has a limited effect on the MBV values of the reconstituted soil. As a result, Soil 4, a mixture composed of 45% sand and 55% kaolinite is selected, corresponding to A1 soil (French standard [33] and having the highest MBV. In following sections, Soil 4 is called as soil-model (SM).

Table 7: Composition of the reconstituted soil-models and corresponding MBV values

Mix	Composition	MBV (g/100g)	% passing at 80 µm (%)	% passing at 2 mm (%)
Soil 1	80% sand + 20% kaolinite	0.5	23	99.82
Soil 2	60% sand + 40% kaolinite	0.7	38	99.64
Soil 3	50% sand + 50% kaolinite	0.8	48	99.83
Soil 4	45% sand + 55% kaolinite	0.8	52	99.75

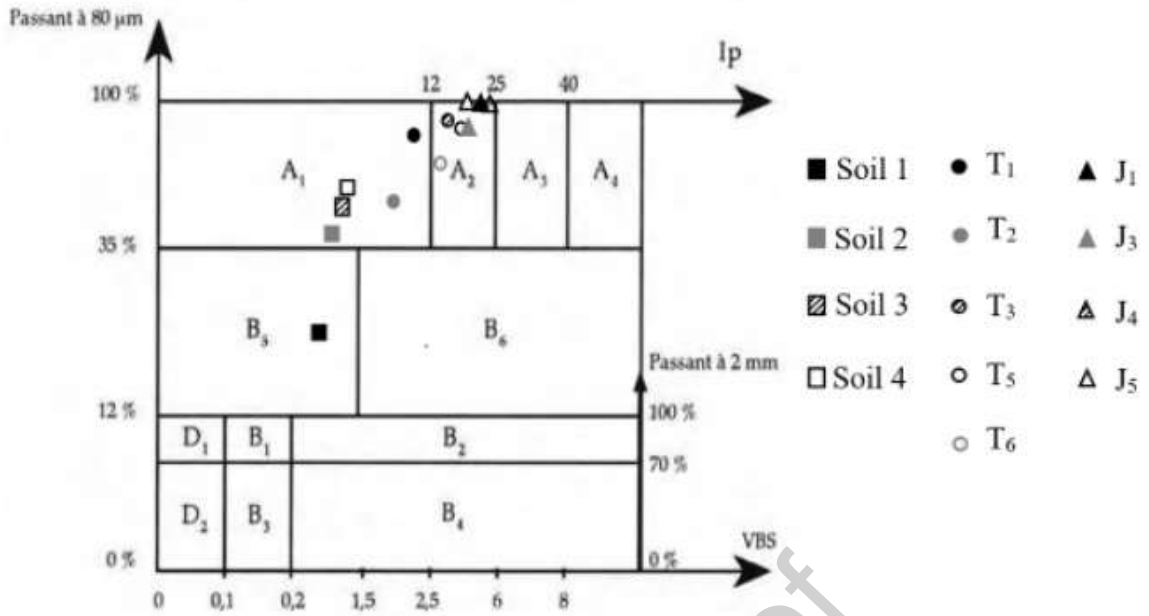

Figure 3: Reconstituted soil-models compared to Usumacinta River raw sediments in GTR chart

The Immediate Bearing Ratio (IBR), which is the value of the immediate CBR index measured on a soil sample compacted to the normal (or standard) Proctor energy without overloading or immersion and with its natural water content, is also measured in accordance with standard [38]. At the optimum water content (OWC ≅ 13%), the IBR is approximately 14% and the dry density ρ_{owc} = 1.78 Mg/ m^3 (Figure 4).

2.2.2. Reconstituted soil-model treated with lime (TSM)

The reconstituted soil-model is treated using quick lime. The lime fixation point (LFP) of Soil 4 is measured as described in Section 2.1.2. The LFP, is equal to 1.5%. For the lime-treated soil, the IBRs are determined at the optimum water content corresponding to the maximum dry density only (Figure 4). In a manner similar to that of sediments, the lime treatment increases the optimal water content from 12.9% to 14.3%. The maximum dry density is unchanged and the IBR index changes from 14.5% to 20.2% (Table 8).

Table 8: Mechanical properties of the soil-model: untreated and the lime-treated

Type of soil-model	Optimum water content w_{owc} (%)	Dry density at OWC ρ_{owc} (Mg/m^3)	IBR (%)
Untreated	12.9	1.78	14.5
Lime-treated	14.3	1.76	20.2

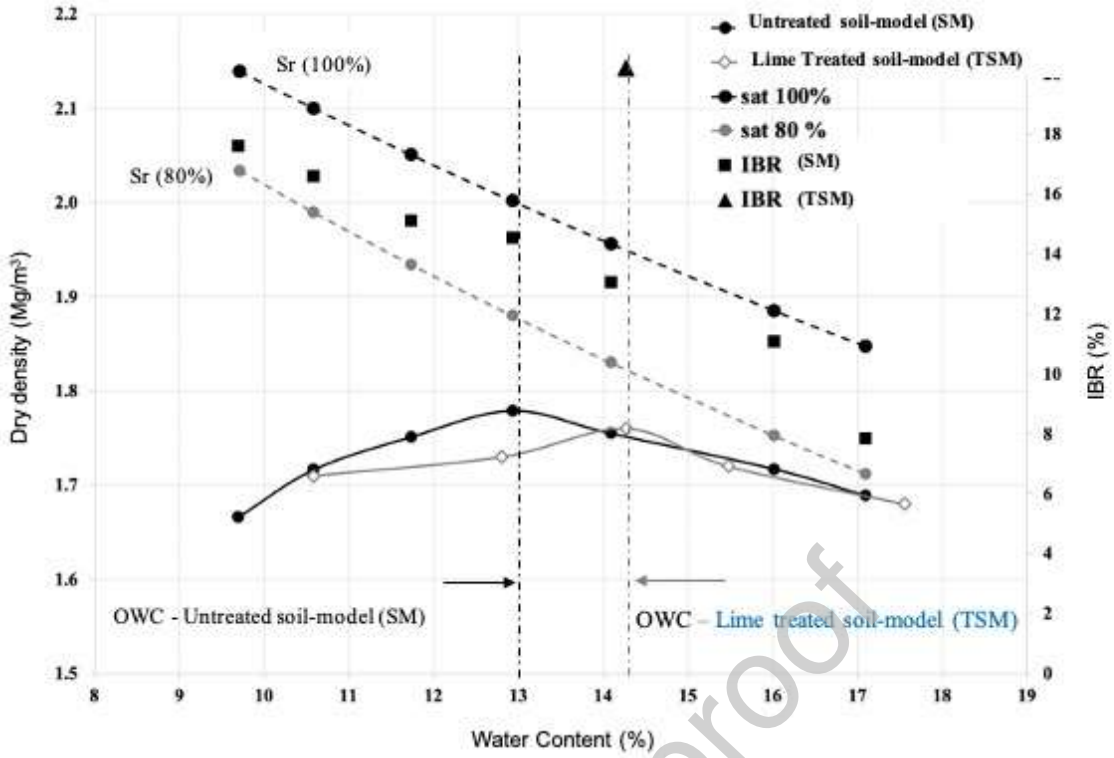

Figure 4 : Proctor - IBR *vs.* water content for the soil-model: untreated (SM) and lime-treated (TSM), (mixture: 45% sand + 55% kaolinite).

2.3. Subgrade material

The full-scale pilot unit requires a large amount of soil material to fill the platform. The subgrade layer, at the bottom of the platform, is filled with raw gravel, with a particle size ranging from 0 to 31.5 mm (GNT 0/31.5), (Cu=20, Cc =5). The gravel material, the most commonly used in France for road construction, is classified as a PG (Poorly graded Gravel) soil according to the Unified Soil Classification System [39].

3. Experimental methodology

3.1. Soil implementation

A 5-m long and 1.8-m wide full-scale unpaved section of road, called the platform in present study, is built in the laboratory. The platform consists of a 0.6 m of gravelly subgrade layer and of a 0.30 m base layer of soil-model. Lightweight non-woven geotextile fabric is placed at the interface between the base and the foundation layers to reduce pollution from the two different layers and to prevent the migration of fine particles from the reconstituted soil-

model till the subgrade layer. The geotextile used is very light, without mechanical resistance to limit the influence on the behavior of the road structure. The foundation layer is reused in both tests.

The whole tested structure is composed of a combination of a subgrade and the based layer on which the loads will be applied.

The subgrade layer is constituted by 0.54 m^3 of gravel material installed in two successive 0.30-m thick layers. Each layer is compacted separately.

The base layer requires careful and rigorous installation. About five tons of dry soil, composed of sand and kaolinite for the untreated soil-model (SM) or of sand, kaolinite, and lime for the treated soil-model (TSM), are mixed per 65 kg steps, to fill the 0.30-m thick base layer. The base layer is implemented in four successive layers to control the homogeneity. The same compaction protocol is used for all the layers. The quantity of material sufficient to obtain a final compacted layer 0.075 m deep over the entire surface of the platform (5 m x 1.8 m), is placed in the container.

The material is previously moistened to the measured optimum water content and compacted with a plate compactor (DENQBAR, DQ-0139) until the target density is reached. After compaction, the height of the compacted soil layer is checked again to determine the exact density of each layer (Table 9). The surface of the compacted soil layer is scarified to ensure better adhesion between the successive ones. The same operation is repeated as many times as the number of layers, i.e. 4 times (Figure 5). Regarding the treated soil-model (TSM), a 21-day air curing period is observed between the installation and testing phases to allow the lime to react with the soil.

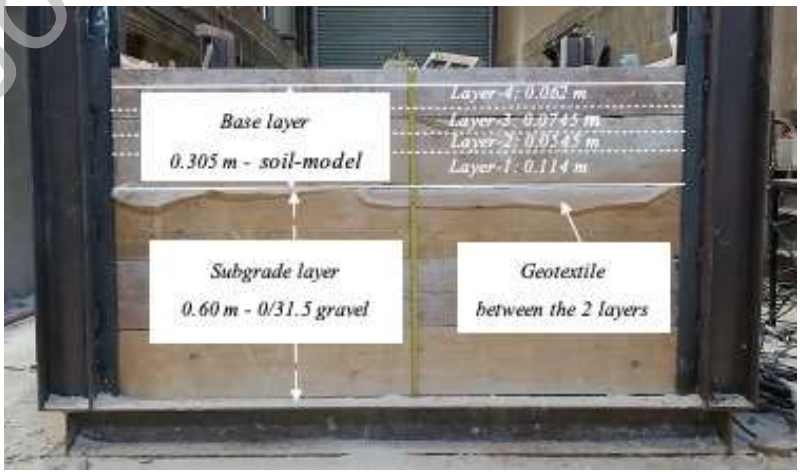

Figure 5: The different layers of the road platform

Table 9: Compaction properties of the untreated and lime-treated soil-models used for the road platform during the implementation

A1 Soil	OWC w_{opt} (%)	Dry density ρ_{owc} at OWC (Mg/m^3)	Wet density (Mg/m^3)
Untreated	13.0	1.78	2.01
Lime-treated	14.3	1.78	2.03

3.2. Quality control

3.2.1. Compaction control

After the installation of the soil base layer, a series of cone penetrometer tests are carried out to control the homogeneity of compaction within the depth and over the entire surface of the experimental road.

Static cone penetrometer tests within the untreated A1 soil base layer

For the untreated soil-model (SM), 24 static cone penetrometer tests are performed according to the French standard [40]. The static cone penetrometer is used to measure the penetration resistance of the soil, which is displayed on a dial in terms of CBR. The values are measured every 38 mm within the depth of the A1 soil base layer. Static cone penetrometer testing is conducted at 24 different locations on the road platform (Figure 6).

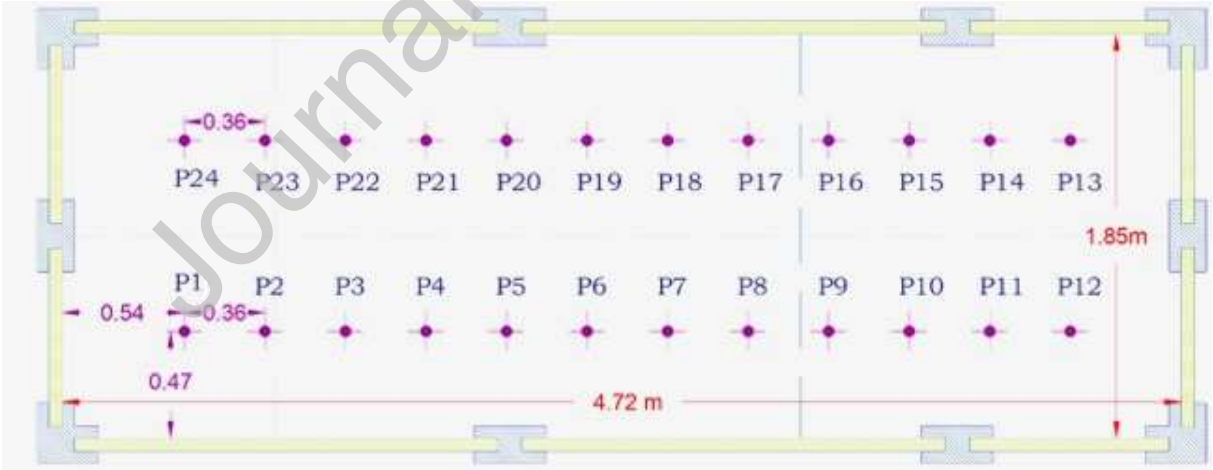

Figure 6: Location of cone penetrometer testing on the road platform.

Dynamic cone penetrometer tests in the lime-treated A1 soil base layer

Considering the gain of cohesion with time for the compacted treated soil, it was decided to use for the lime-treated soil-model (TSM), the TRRL DCP (Dynamic Cone Penetrometer A2465). The test consists in introducing a cone into the soil by dropping a weight. For each

weight drop, the CBR is obtained through a correlation relating the penetration resistance to CBR values. Dynamic cone penetrometer testing is conducted through the entire thickness of the lime-treated soil.

3.2.2. Bearing Capacity of untreated and lime-treated soil-models after compaction

CBR values are measured at 24 different locations on the soil base layer (Figure 6) and every 0.038 m through the full thickness of the layer. The average CBR value of all these measurements is 2.8, which is relatively low but in line with the values usually obtained for clayey materials. Regarding the vertical homogeneity, an increase in the CBR values is observed at a depth between 0.15 and 0.26 m.

Noticed that the deeper layers are more compacted than the upper ones. This can be explained by the fact that the lowest layer receives the cumulative compaction effort of the upper layers. As a result, the untreated soil-model (SM) has a lower strength in the first 0.15 m from the surface with an average CBR value of 2.1 and is more resistant in the deeper layers with an average CBR value of 3.7 at a depth from 0.15 m to 0.26 m (

Figure 7).

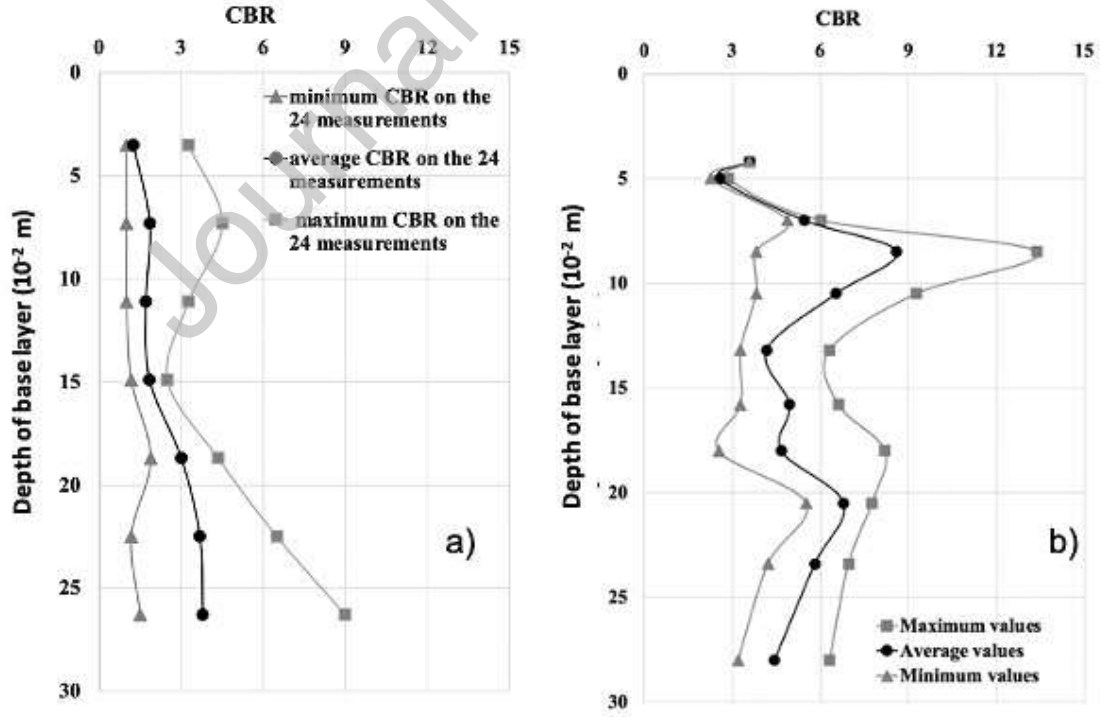

Figure 7: CBR profiles obtained with static cone penetrometer tests in the untreated soil-model - SM base layer (left), and profiles obtained with the dynamic cone penetrometer in the lime-treated soil-model – TSM (right)

The average CBR value of all the measurements obtained at the platform surface and through the whole thickness of the treated soil-model - TSM layer is 5.3. CBR values are higher around a depth of 0.07 m and 0.20 m, respectively. This trend demonstrates clearly the effect of the lime treatment.

3.2.3. Surface level control

The test platform is subdivided into a plate test section and a traffic section. The testing area dedicated to cyclic plate loading testing, is 1.8 m wide, 1.9 m long and 1.1 m high (see Section 3.3.1). The second area, which corresponds to a full length of circulated road platform of 3 m with an effective length of 2 m, is for traffic load testing (see Section 3.3.2).

The laser displacement sensors move along the lines to map the surface condition of the soil. Measurements are made in two steps, before loading and after plate and traffic tests, in order to evaluate the level of generated deformation. Four laser sensors are mounted on a fixed bar moved to various locations on the platform for the traffic loading test area and one other 5 for the plate loading test.

3.3. Full scale testing

3.3.1. Cyclic plate vertical loading test

The test consists of applying a cyclic load using a rigid steel plate (Figure 8a). The plate has the shape of a wheel footprint, i.e., a rectangle 180 mm long, closed at both ends by arcs. The plate is 3 cm thick with a surface area of 0.043 m^2. According to AASHTO [41], the damaging effect of the passage of an axle of any mass can be represented by an Equivalent Single Axle Loads or ESAL load as:

$$ESALs = N \times \left(\frac{Load}{40kN}\right)^4 \quad (1)$$

where N is the number of loading cycles [42].

The maximum load applied to the platform surface is 40 kN, so that each cycle corresponds to one ESAL. Each loading cycle, therefore, corresponds to a single ESAL with an applied pressure of 930 kPa. Cyclic loading is applied at a constant frequency up to 1 Hz, as specified in the published AASHTO standard [43],. The cyclic load signal is generated using a hydraulic loading system. The maximum load is applied during 0.2 s, the unloading phase

lasts 0.5 s, and the loading-unloading phases are completed in 0.6 s [44]. Each cycle of the plate loading test is considered as one ESAL run. The plate can apply 1,500 cycles to the base layer soil. During testing, the vertical load applied to the soil base layer and the surface displacement of the soil are measured and recorded.

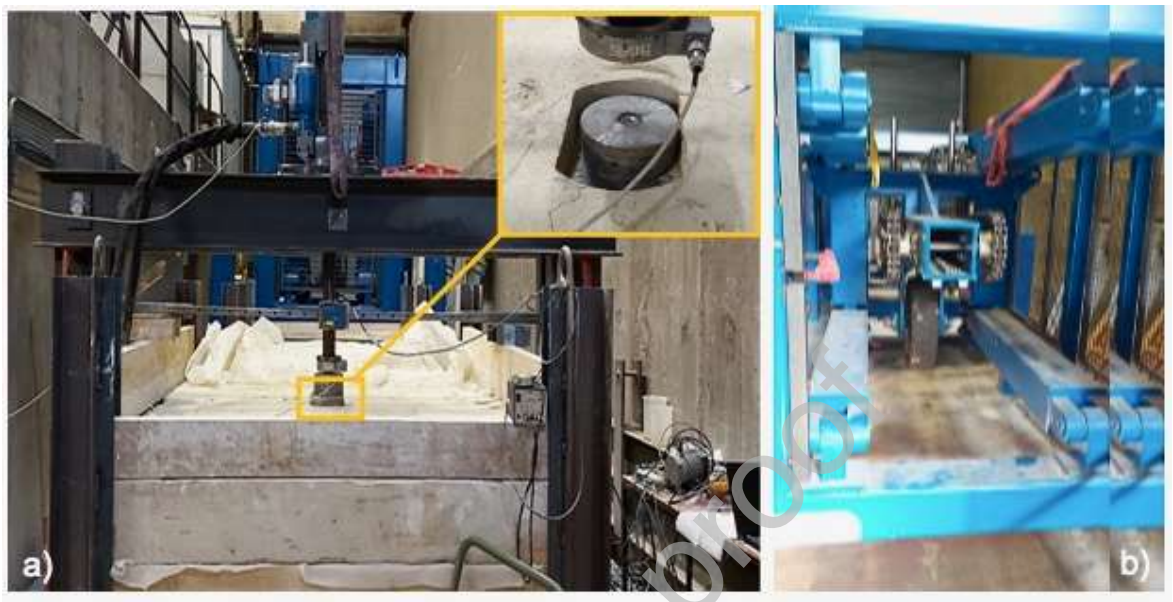

Figure 8: (a) Global view of the cyclic plate loading test device: support beam, hydraulic jack and plate, (b) Traffic load simulation on the road platform

3.3.2. Traffic load testing

Traffic load is applied using a full-scale device that simulates unidirectional traffic under normal loading corresponding to a load of a half axle (Equivalent Single Axle Loads [41]. The pneumatic wheel is mounted on a specific device [44]. The dimensions of this device are 4.5 m long, 1.8 m wide and 2.3 m high, with a total mass of 8,400 kg. The one-way traffic is simulated using an 86-kg tire of 0.18 m in width and 0.78 m in diameter (Figure 8b). The device permits contact stress of 650 kPa to be applied to the wheel-surface of the soil. The load is applied to the wheel via the self-weighing device and then controlled by two pneumatic jacks. The main beam is attached to a deformable parallelogram to apply the same load whatever the position of the tire, and make sure that the same load magnitude is applied to the road platform surface even after extensive rutting appears. The wheel speed is 7 km/h and 1,500 traffic cycles can be applied on the platform. At the end of the test, the displacement profile is measured at different positions in the plane perpendicular to the direction of traffic, using a laser sensor.

4. Results

4.1. Untreated soil-model (SM)

Plate testing

The target value of plate vertical testing was 40 kN. The measured loading level reached was 12.5 kN, giving 12.5/40=31.25% of the set point (Figure 9a). This difference results from the low compactness of the untreated soil-model (SM), as expected. Finally, the settlement stabilized at 0.12 m corresponding to its course (Figure 9b). By adding a metal support of 0.1 m in the rut, the experiment was continued (Figure 9c), reaching a displacement of about 0.215 m (Figure 9d).

As a result, the untreated soil-model (SM) presents a total settlement of 0.21 m after 7 cycles.

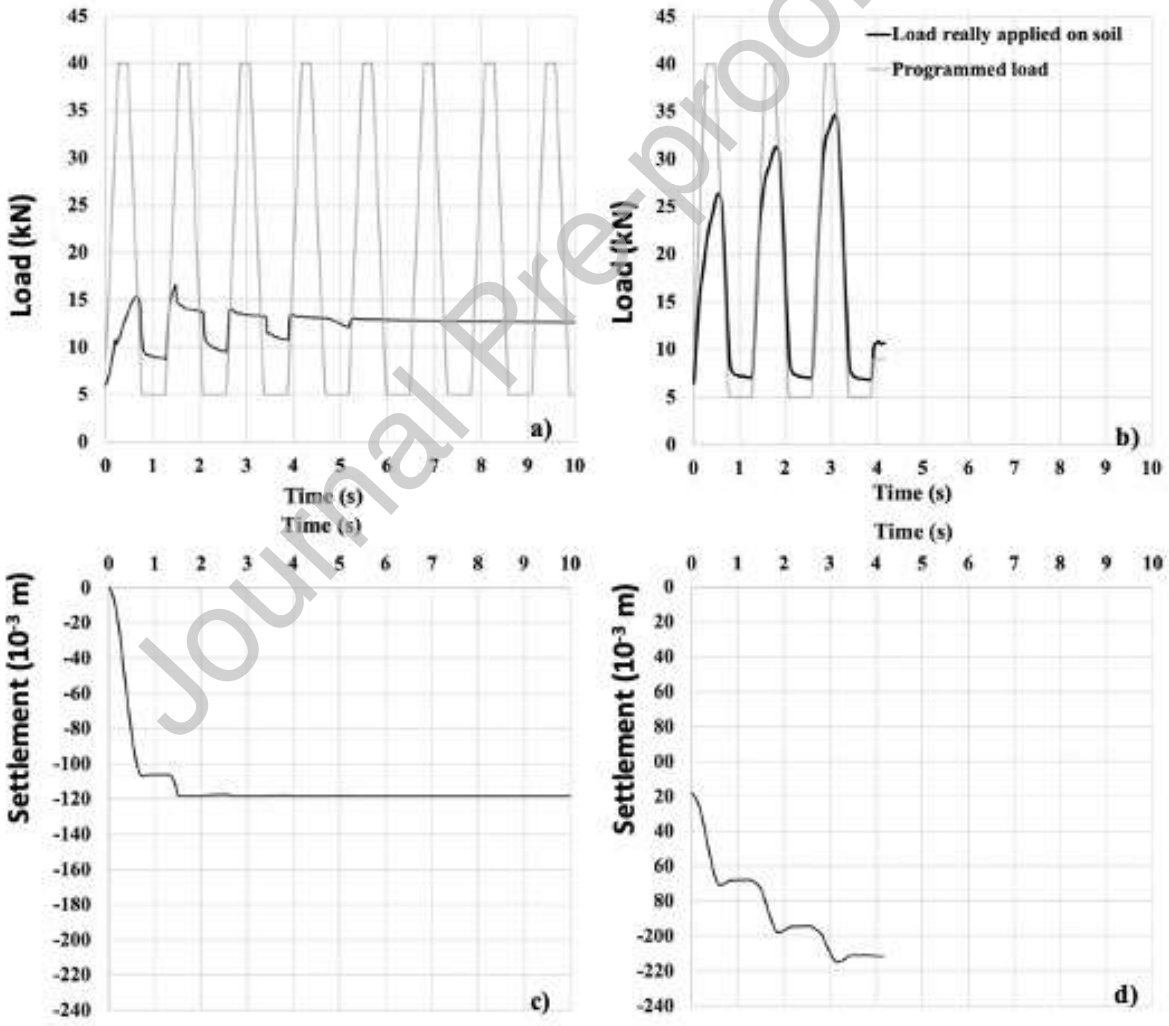

Figure 9: Plate testing on the untreated soil-model base layer: (a) first four loading cycles; (b) 5th to 7th loading cycles; (c) settlement during the first four cycles; (d) settlement observed during 5th to 7th cycles

The soil level trend before the beginning of the test is approximately linear across the full 2-m width (Figure 10).

The surface level raises slightly (0.022 m). After 7 plate test cycles, the soil settlement reaches 0.21 m. Heaving or punching are localized around the point of application of the plate.

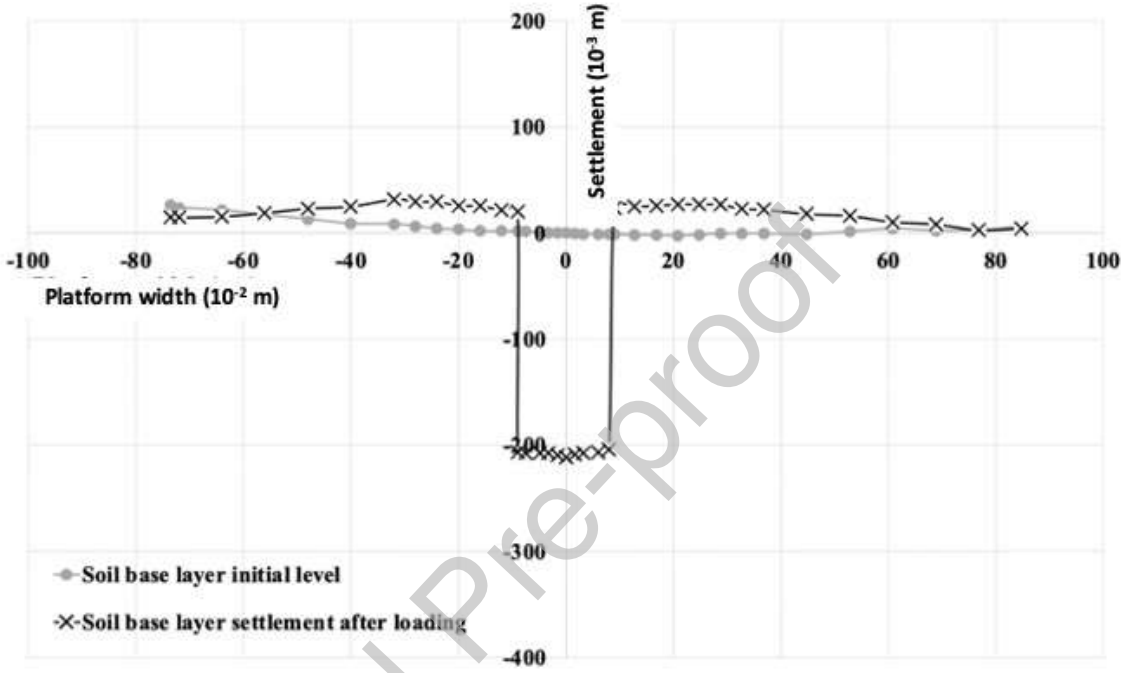

Figure 10: Untreated soil-model (SM) base layer settlement profile before and after plate testing

Full scale traffic load testing

Before traffic load testing, the soil base layer surface is approximately plane as expected. Differences in surface levels present a low differential range between 0.02 and 0.04 m.

The tests are stopped after 1,200 load cycles when extensive rutting developed and the boundary limits of the machine have been reached. After 1,200-wheel passes, a rut 0.17 m deep is observed. On both sides of the tire, the soil rises by about 0.09 m. Despite a tire width of 0.18 m, the rut width is 0.29 m on the soil surface, which is 1.6 times larger than the tire. The wheel range of action is 0.60 m, since beyond this distance from the center, the profiles of the before and after test soil surfaces overlap and the effect of traffic loading become negligible (Figure 11). Settlement is measured at three different equidistant locations. Settlement overlapping demonstrates that the impact of the tire is homogeneous over the

entire surface (Figure 11). Figure 12 shows a 3-D view of rutting after completion of the traffic test. The colours change depending on the rut depth. Raised soil level on both sides of the rut appears in yellow.

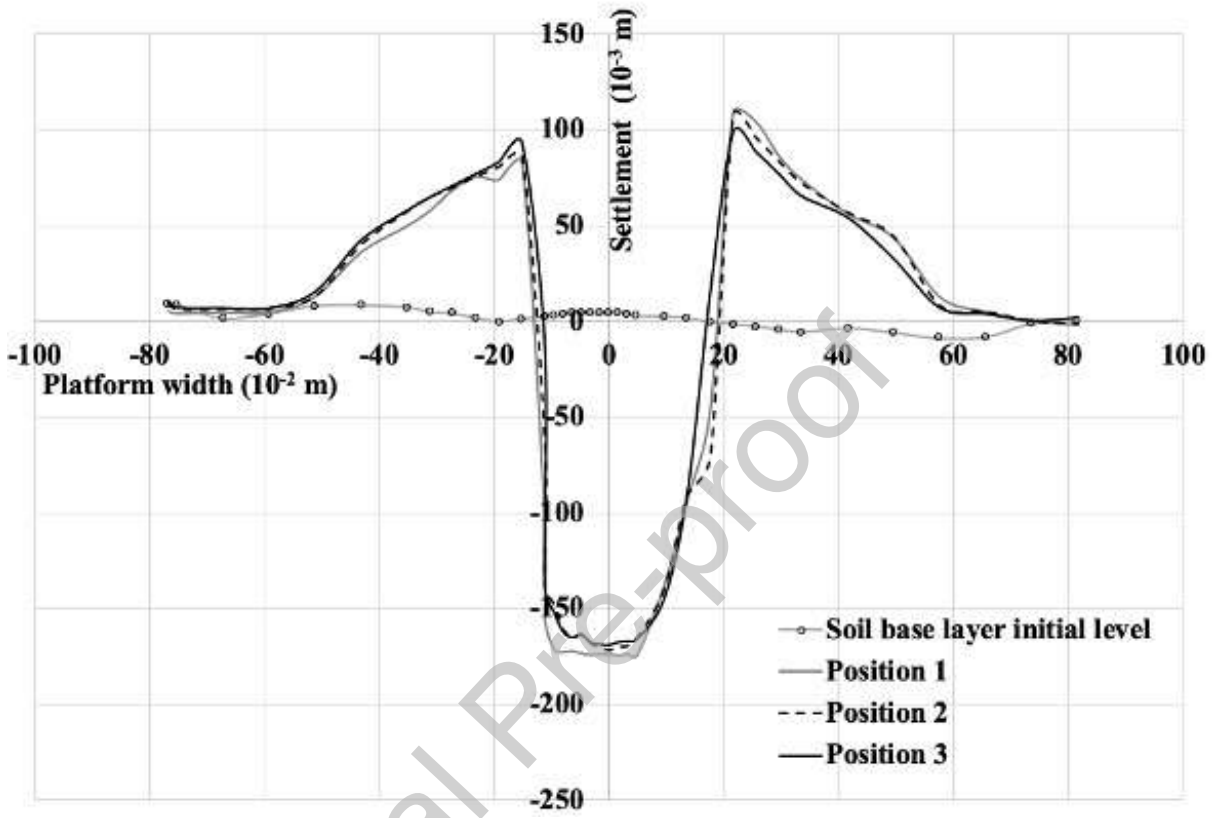

Figure 11: Untreated soil-model (SM) base layer profiles before and after traffic load testing

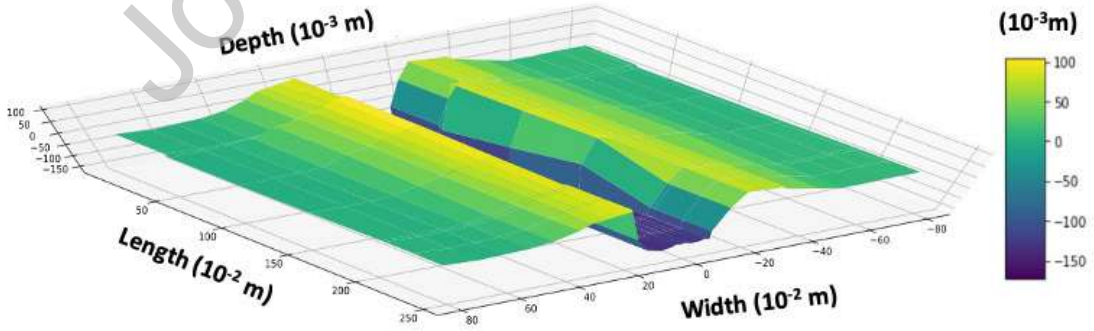

Figure 12: 3-D view of the rut profile after traffic load testing on the untreated soil-model (SM) base layer

4.2. 440Lime-treated soil-model (TSM) compared to untreated soil-model (SM)

Plate testing

A maximum settlement of 0.39 m is reached after 1,500 load cycles applied to the lime-treated soil-model -TSM (Figure 13). Figure 14 displays the soil base layer settlement profiles before and after cyclic plate testing. The soil surface before testing is quasi-horizontal with some irregularities within +/- 0.015 m at the edges of the platform. The settlement value reaches 0.39 m. On both sides of the plate, the soil rises by 0.05 to 0.10 m.

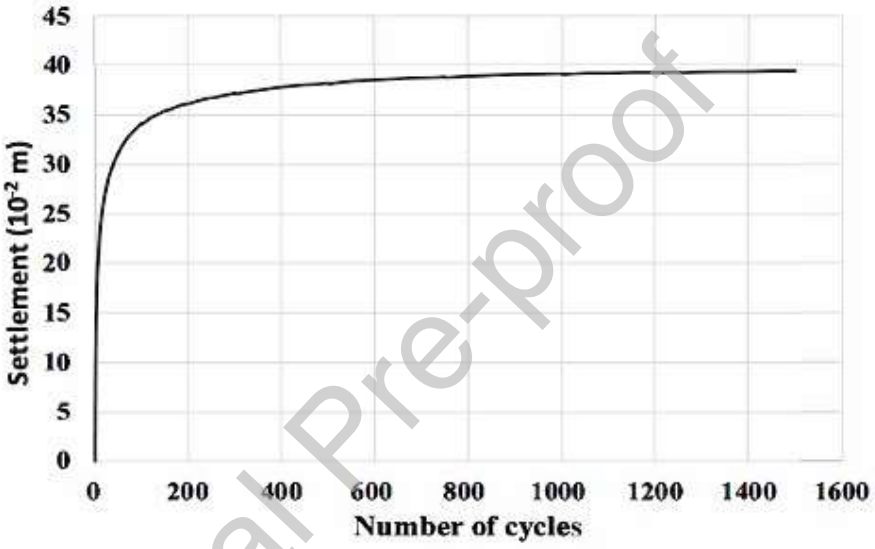

Figure 13: Lime-treated soil-model (TSM) base layer settlement versus the number of cycles during plate testing

Soil behavior under plate testing conditions

The plate tests are conducted on both types of soil-models. As regards the untreated soil-model (SM), only seven loading cycles have been applied (Figure 9), whereas the lime-treated soil-model (TSM) has supported 1,500 loading cycles. The final plate footprint depth for the lime-treated soil-model (TSM) is greater (0.39 m) than that for the untreated soil-model (SM) but it can withstand as much as 300 times more loading cycles (Figure 14). Consequently, although the depth remains significant for the lime-treated soil-model (TSM), the treatment has substantially improved the soil characteristics. In both cases, soil raising can be observed on both sides of the plate. This elevation is smaller and spreads over a wider surface for the untreated soil-model (SM), while it is steeper for the lime-treated soil-model (TSM).

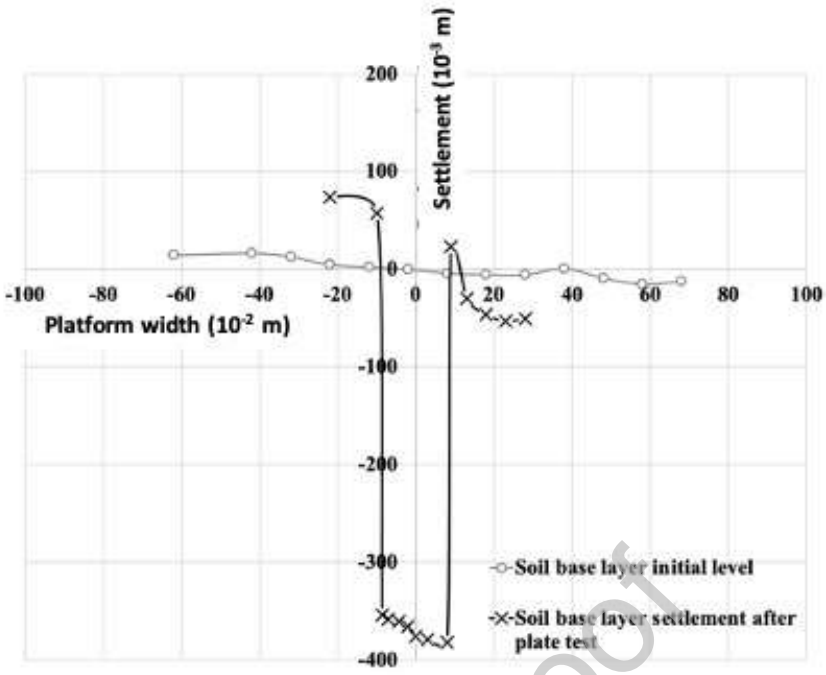

Figure 14: Lime-treated soil-model (TSM) base layer settlement profile before and after plate testing

Full scale traffic load testing

During the first wheel passes, rutting increases rapidly and stabilizes around the 600th pass to reach a maximum rutting value of 0.13 m (Figure 15). The soil base layer settlement profile after 1,500 passes is shown in Figure 16. As abovementioned, the rut depth is measured using some laser sensors mounted on a rigid beam. At the end of the test, the rut depth is approximately 0.14 m after 1,500 passes, which corresponds to the displacement measured during the test in Figure 15. On both sides of the rut, the maximum raise is equal to 0.013 m. With 1.5% lime, the gain in rutting deep is 25%, from 0.175 m to 0.140 m, for untreated and lime-treated soil-models respectively, and the same number of passes: 1,500 (Figure 17).

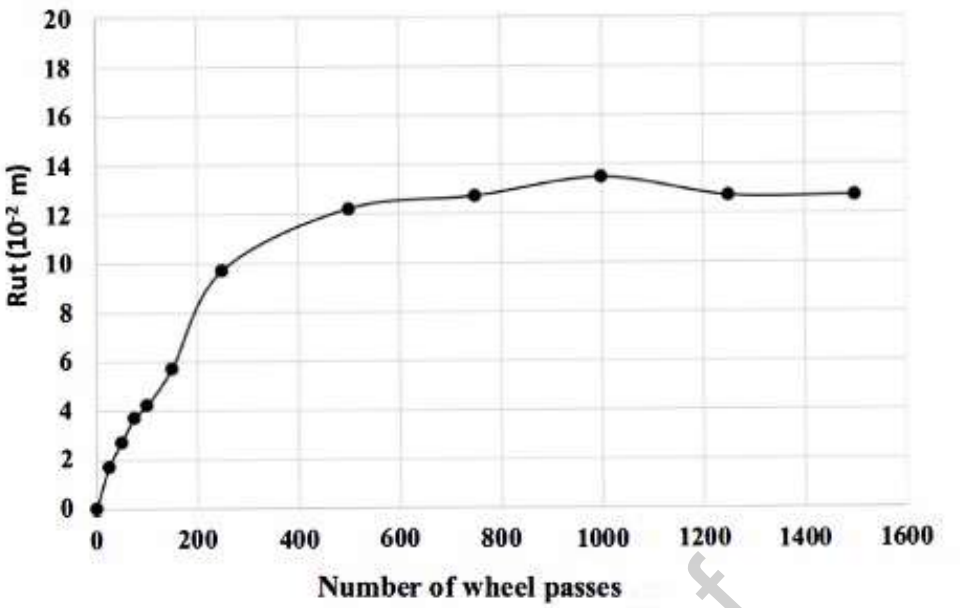

Figure 15: Rut depth versus the number of wheel passes

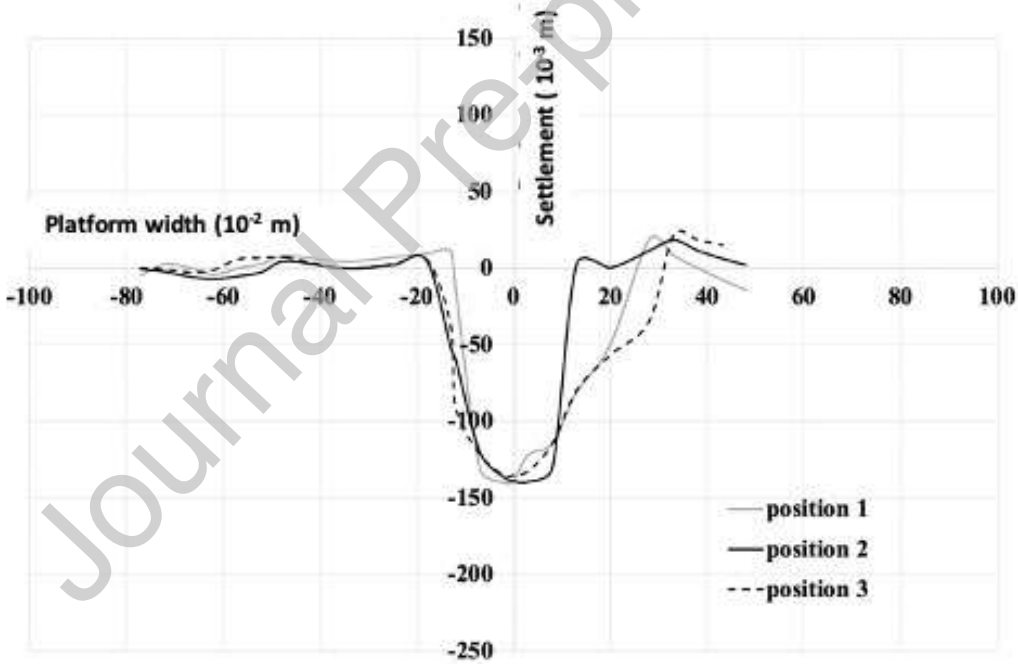

Figure 16: Comparison of the soil-model base layer rut profiles after traffic load testing at the three locations of the laser sensors

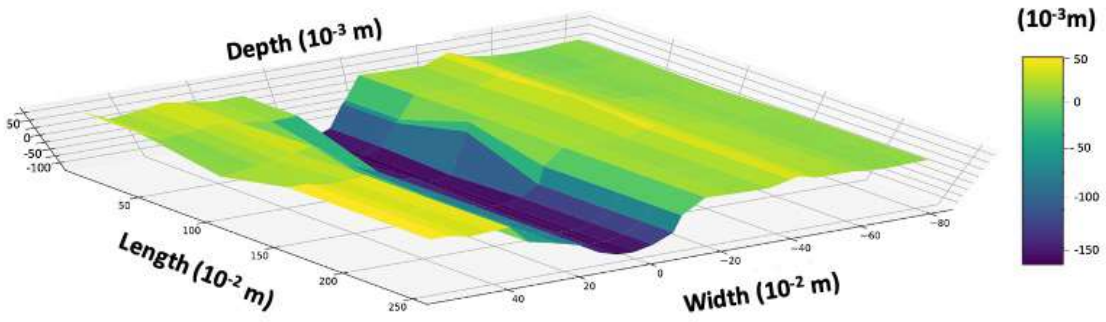

Figure 17: 3-D view of the rut profile after traffic load testing on the lime-treated soil-model (TSM).

Soil behavior under traffic load testing conditions

Considering the traffic load testing, the untreated soil-model (SM) presents a depth rut of 0.17 m after 1,200 load cycles. The 1,500 programmed passes, have been carried out for the lime-treated soil-model (TSM). The final depth rut obtained is less than 0.14 m.

The raise of the soil surface is the distance between the soil surface before the test and the highest soil heave after testing. Also at the surface level, the lime treatment significantly reduces heave (0.10m for the untreated soil-model (SM) instead of 0.02 m for the treated (TSM) one).

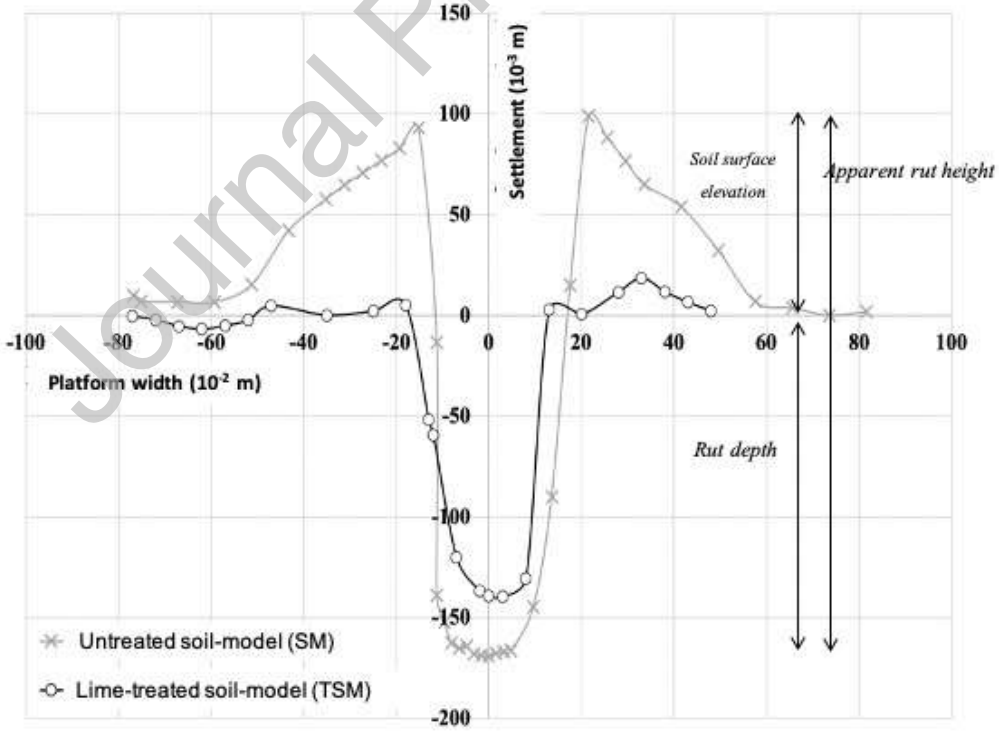

Figure 18: Comparison between the untreated and lime-treated soil-models base layer rut profiles after traffic load testing

As shown just above on Figure 18, the lime treatment improves the characteristics of soil-model. The soil can withstand more cyclic loads and the height of the apparent rut is significantly reduced during traffic load testing. Rutting, however, remains significant in both cases: 0.265 m and 0.145 m for untreated and lime-treated soil-models respectively (Figure 18).

5. Synthesis

The geotechnical identification of the Usumacinta sediments shows that they belong mostly to the A1 class (including A2).

A soil-model, consisting of Hostun sand and kaolinite (Figure 3) implemented and this soil-model is replicable under controlled conditions. Among different mixes of sand and kaolinite tested, one of them presents similar geotechnical properties of untreated soil-model (ρ_{owc}, w_{owc}, CBR) as the raw sediments: this mix selected for full-scale experiments, called soil-model was used without treatment (no lime, SM) and with lime (treated soil-model, TSM)

The soil-model (SM) was also treated with low lime concentration (1.5%).

The full-scale pilot experiments are proposed to highlight the positive effect of lime treatment.

The results are satisfactory: (i) the addition of lime makes it possible to reinforce the CBR close to the surface of the compacted soil; (ii) the soil treated under cyclic vertical plate loading withstands more loading cycles reducing the permanent deformation; (iii) the lime treatment significantly reduces the rutting generated by a wheel representing a horizontal cyclic axle loading of 11 tons.

These results are very encouraging and demonstrate the potential for transferring the study's contributions to Usumacinta River sediments. The potential to use sediments for unpaved road construction has multiple positive impacts on resource preservation, economic activity development, and the quality of life and activities of riverside populations.

6. Conclusions

The valorisation of the Usumacinta River sediments for the construction of unpaved roads with earth layers have an impact on the economic well-being of the state of Tabasco, Mexico, since many local activities are highly dependent on an adequate all-weather road network.

Based on full-scale cyclic plate load and traffic loading tests conducted on two reconstituted soils (untreated and treated) with characteristics close to those of the raw sediments, the following conclusions can be drawn:

The geotechnical characteristics and mechanical properties of the Usumacinta River sediments have been determined. A lime treatment increased the mechanical properties significantly (MDD, OWC). The use of local lime would have an economic and environmental impact because transportation costs would be reduced. The full-scale results of the cyclic plate and traffic load testing, demonstrate accurately, that the lime tρeatment improves the immediate soil performance and lengthens the service life of the unpaved road.

The present study, including full-scale testing with realistic loads, demonstrates promising results related to the sustainable and beneficial use of river sediments as a natural resource. Recycling river sediments to build local earth unpaved roads would provide major support for the people living along the river, especially since river banks are not protected and local roads are regularly flooded. Whether for construction or maintenance, the use of local sediments could have a positive socio-economic impact on the riverside population.

Declaration of interests

Irini Djeran-Maigre reports financial support was provided by French National Research Agency. Irini Djeran-Maigre reports a relationship with National Institute of Applied Sciences of Lyon that includes: funding grants. non conflict of interest

Acknowledgements

The funds for this study work have been provided within the context of the joint research project “From traditional uses to an integrated valorisation of sediments in the Usumacinta River basin (VAL-USES)” by the Agence Nationale de la Recherche of France (ANR-17-CE03-0012-01) and the Consejo Nacional de Ciencia y Tecnología of Mexico (FONCICYT-290792).

The authors would like to thank the staff of INSA Lyon for its technical support: S. Vacherie, E. Bruyère, J. Laforet; to thank also O. Linares, W. Sabalbal, I. Lipatoff, Master students and A. Valogiannis, PhD student at INSA Lyon as well as R. Del Negro, Master student from INSA and the University of Nantes and M. Hussain, PhD student from the University of Caen, Normandie.

References

[1] VAL-USES, 2017. From traditional uses to an integrated valorization of sediments in the Usumacinta River basin – VAL-USES. ANR-17-CE03-0012, https://anr.fr/Project-ANR-17-CE03-0012

[2] World Bank, 2020, Rural population. World Bank staff estimates based on the United Nations Population Division's World Urbanization Prospects: 2018 Revision. https://data.worldbank.org/indicator/SP.RUR.TOTL.ZS?view=map

[3] World Bank, 2008. Transport for Development. The World Bank Group. 113.

[4] M.P.N. Burrow, H. Evdorides, G.S. Ghataora, R. Petts, M.S. Snaith, The evidence for rural road technology in low-income countries. Proceedings of the Institution of Civil Engineers: Transport 169, (2016) 366–377. https//doi.org/10.1680/jtran.15.00089

[5] E. Ngezahayo, G.S. Ghataora, M.P.N. Burrow, Factors affecting erosion in unpaved roads. World Congress on Civil, Structural, and Environmental Engineering (2019) 1–9. https://doi.org/10.11159/icgre19.108

[6] C.E. Ramos Scharrón, Sediment production from unpaved roads in a sub-tropical dry setting – Southwestern Puerto Rico. Catena, 82, (2010) 146-158, doi:10.1016/j.catena.2010.06.001

[7] I.G Kavouras., D.W. Dubois, G. Nikolich, A.Y. Corral Avittia, V. Etyemezian, Particulate dust emission factors from unpaved roads in the U.S.-Mexico border semi-arid region. Journal of Arid Environments 124, (2016) 189–192. https://doi.org/10.1016/j.jaridenv.2015.07.015

[8] A.D. Ziegler, R.A Sutherland., T.W. Giambelluca, Interstorm surface preparation and sediment detachment by vehicle traffic on unpaved mountain roads. Earth Surface Processes and Landforms 26, (2001) 235–250. https://doi.org/10.1002/1096-9837(200103)26:3<235:AID-ESP171>3.0.CO;2-T

[9] C.P. Crossley, V.N. Kibiwo., A.J. Reynolds, R.J. Rickson, Rut formation and rolling resistance on earth roads. Journal of Agricultural and Engineering Research 78, (2001)99–107. https://doi.org/10.1006/jaer.2000.0634

[10] R. Hufenus, R. Rueegger, R. Banjac, P. Mayor, S. Springman, R. Brönnimann, Full-scale filed tests on geosynthetic reinforced unpaved roads on soft subgrade. Geotextiles and Geomembranes, 25, (2006) 21-37. doi:10.1016/j.geotexmem.2005.06.002

[11] N. Khoueiry, L. Briançon, A. Daouadji, A. Abdelouhab, (2019) Laboratory test on agregats geosynthetic reinforcement for unpaved roads on soft subgrade applications. Proceedings of the XVII ECSMGE, Reykjavik, doi: 10.32075/17ECSMGE-2019-0075

[12] World Bank, 2018. Championing adaptation in Mexico: protecting communities from the impacts of climate change. Rural population. https://www.worldbank.org/en/results/2018/07/25/promover-la-adaptacion-en-mexico

[13] J. Lebo, D. Schelling, (2001) Design and Appraisal of Rural Transport Infrastructure, ensuring basic Access for rural communities. World Bank technical Paper, n°496. https://doi.org/10.1177/0019556120010319

[14] B. Blankespoor, T. Bougna, R. Garduno-Rivera, H. Selod, (2017) Roads and the Geography of Economic Activities in Mexico. World Bank Group, Development Research Group Environment and Energy Team & Development Data Group. Policy Research Working Paper, n°8226. https://doi.org/10.1596/1813-9450-8226

[15] CIA, 2019. The World Factbook : Roadways 5–5. https://doi.org/10.18356/9a7e0002-en

[16] V. Dubois, N.E. Abriak, R. Zentar, G. Ballivy, The use of marine sediments as a pavement base material. Waste Management 29, (2009) 774–782 doi.org/10.1016/j.wasman.2008.05.004

[17] T. Chompoorat, T. Thepumong, S. Taesinlapachai, S. Likitlersuang, Repurposing of stabilised dredged lakebed sediment in road base construction. Journal of Soils and Sediments (2021) 21:2719–2730. https://doi.org/10.1007/s11368-021-02974-3

[18] A. Maher, 2005. Geotechnical testing and beneficial reuse evaluation of river sediments palmyra cove demonstration project. Final report. State of New Jersey Department of Transportation Office of Maritime Resources and U.S. Department of Transportation Federal Highway Administration. 49p.

[19] W. Maherzi, M. Benzerzour, Y. Mamindy-Pajany, E. van Veen, M. Boutouil., N.E. Abriak, Beneficial reuse of Brest-Harbor (France)-dredged sediment as alternative material in road building: laboratory investigations. Environmental Technology (United Kingdom) 39, (2018) 566–580. https://doi.org/10.1080/09593330.2017.1308440

[20] S. Kamali, F. Bernard., N.E. Abriak, P. Degrugilliers, Marine dredged sediments as new materials resource for road construction. Waste Management 28, (2008) 919–928. https://doi.org/10.1016/j.wasman.2007.03.027

[21] D. Levacher, D. Colin, A.C. Perroni, Z. Duan, L. Sun, Recyclage et valorisation de sédiments fins de dragage à usage de matériaux routiers (2006) 603–612. https://doi.org/10.5150/jngcgc.2006.058-l

[22] D. Wang, N.E. Abriak, R. Zentar, Dredged marine sediments used as novel supply of filling materials for road construction. Marine Georesources and Geotechnology 35, (2017) 472–480. https://doi.org/10.1080/1064119X.2016.1198945

[23] N. Yoobanpot, P. Jamsawanga, H. Poorahong, P. Jongpradist, S. Likitlersuang, Multiscale laboratory investigation of the mechanical and microstructural properties of dredged sediments stabilized with cement and fly ash. Engineering Geology 267 (2020) 105491. https://doi.org/10.1016/j.enggeo.2020.105491

[24] A. Loudini, M. Ibnoussina, O. Witam, A. Limam, O. Turchanina, 2020. Valorisation of dredged marine sediments for use as road material. Case Studies in Construction Materials 13. https://doi.org/10.1016/j.cscm.2020.e00455

[25] D.X. Wang, N.E. Abriak, R. Zentar, W. Xu, Solidification/stabilization of dredged marine sediments for road construction. Environmental Technology 33, (2012) 95–101. https://doi.org/10.1080/09593330.2011.551840

[26] R. Zentar, H. Wang, D. Wang, 2021. Comparative study of stabilization/solidification of dredged sediments with ordinary Portland cement and calcium sulfo-aluminate cement in the framework of valorization in road construction material. Construction and Building Materials 279. https://doi.org/10.1016/j.conbuildmat.2021.122447

[27] A. Furlan, A. Razakamanantsoa, H. Ranaivomanana, A. Ouali, D. Levacher, D. Deneele, 2021. Effect of fly ash on microstructural and resistance characteristics of dredged sediment stabilized with lime and cement. Construction and building materials. V. 272, 121637, https://doi.org/10.1016/j.conbuildmat.2020.121637

[28] P. Jamsawang, S. Charoensil, T. Namjan, P. Jongpradist, S. Likitlersuang, Mechanical and microstructural properties of dredged sediments treated with cement and fly ash for use as road materials. Road Materials and Pavement Design. (2020) https://doi.org/10.1080/14680629.2020.1772349

[29] A. Furlan, A. Razakamanantsoa, H. Ranaivomanana, D. Levacher, T. Katsumi, Shear strength performance of marine sediments stabilized using cement, lime and fly ash. Construction and building materials. V.184, (2018) 454-463. https://doi.org/10.1016/j.conbuildmat.2018.06.231

[30] R. Zentar, V. Dubois, N.E. Abriak, Mechanical behaviour and environmental impacts of a test road built with marine dredged sediments. Resources, Conservation and Recycling 52, (2008) 947–954. https://doi.org/10.1016/j.resconrec.2008.02.002

[31] R. Achour, N.E. Abriak, R. Zantar, 2014. Valorization of unauthorized sea disposal dredged sediments as a road foundation material. Environmental Technology (United Kingdom) 35, 1997–2007. https://doi.org/doi.org/10.1080/09593330.2014.889758

[32] JORF, Journal officiel de la République Française, 2006. Arrêté du 09/08/2006 relatif aux niveaux à prendre en compte lors d'une analyse de rejets dans les eaux de surface ou

de sédiments marins, estuariens ou extrait de cours d'eau ou canaux relevant respectivement des rubriques 2.2.3.0 ; 4.1.3.0 et 3.2.1.0 de la nomenclature annexée au décret n°93-743 du 29 mars. N°222, 24 septembre 2006.

[33] NF P 11-300, 1992. Earthworks. Classification of materials for use in the construction of embankments and capping layers of road infrastructures.

[34] NF P 94-093, 2014. Soils: investigation and testing – determination of the compaction reference values of a soil type – standard Proctor test – modified Proctor test

[35] V. Dubois, 2006. Étude du comportement physico-mécanique et caractérisation environnementale des sédiments marins – valorisation en technique routière. PhD thesis. Université d'Artois, 285p., https://www.sudoc.fr/103524967

[36] ASTM D6276, 2019. Standard test method for using pH to estimate the soil-lime proportion requirement for soil stabilization

[37] I. Djeran-Maigre, Ph. Dubujet, T.M. Vogel, Variation over time of excavated soil properties treated with surfactants, *Environmental Earth Sciences*, (2018) 77(3) https://dx.doi.org/10.1007/s12665-018-7230-z

[38] NF P 94-078, 1997. Soils: investigation and tests – CBR immersion – Immediate CBR - Immediate bearing ratio – measurement on sample compacted in CBR mould.

[39] ASTM D2487-17E1, 1997. Standard practice for classification of soils for engineering purposes (Unified Soils Classification System).

[40] NF P 94-113, 1996. Soil: investigation and testing – cone penetration test.

[41] AASHTO, 1993. Guide for design of pavement structures. American Association of State Highway and Transportation Officials. 624p.

[42] M. Abu-Farsakh, S. Hanandeh, L. Mohammad, Q. Chen, Performance of geosynthetic reinforces/stabilized paved roads built over soft soil under cyclic plate loads. Geotextiles and Geomembranes. 44, (2016)845-853. http://dx.doi.org/10.1016/j.geotexmem.2016.06.009

[43] AASHTO, 2001. Guidelines for geometric design of very low-volume local roads (ADT<400). American Association of State Highway and Transportation Officials. 72p.

[44] N. Khoueiry, 2020. Study of granular platforms behaviour over soft subgrade reinforced by geosynthetics: experimental and numerical approaches. PhD Thesis. INSA, Lyon, April 16th, 229p.